REPORT DOCUMENTATION PAGE

Form Approved
OMB NO. 0704-0188

1. AGENCY USE ONLY *(Leave blank)*	2. REPORT DATE	3. REPORT TYPE AND DATES COVERED
	3/14/1997	Final Progress Report 5/1/1995-12/31/1996

4. TITLE AND SUBTITLE
LDA MEASUREMENTS OVER AN OSCILLATING RECTANGULAR WING

5. FUNDING NUMBERS
DAAH04-95-1-0170

6. AUTHOR(S)
B.R. Ramaprian

7. PERFORMING ORGANIZATION NAME(S) AND ADDRESS(ES)
Washington State University, Pullman, WA 99164

8. PERFORMING ORGANIZATION REPORT NUMBER

9. SPONSORING / MONITORING AGENCY NAME(S) AND ADDRESS(ES)
U.S. Army Research Office
PO Box 12211
Research Triangle Park, NC 27709-2211

10. SPONSORING / MONITORING AGENCY REPORT NUMBER
ARO 33857.3-EG

11. SUPPLEMENTARY NOTES
The views, opinions and/or findings contained in this report are those of the author(s) and should not be construed as an official Department of the Army position, policy or decision, unless so designated by other documentation.

12a. DISTRIBUTION / AVAILABILITY STATEMENT
Approved for public release; distribution unlimited.

12b. DISTRIBUTION CODE

13. ABSTRACT *(Maximum 200 words)*
Experimental results of measurement of the phase-locked velocity distributions in the three-dimensional vortical region over the tip region of a rectangular wing oscillating sinusoidally about its quarter-chord axis are reported. The tests were conducted in a low-speed wind tunnel at a Reynolds number of 350,000 and velocity measurements were made using a three-component Laser Doppler Anemometer (LDA). The wing was oscillated at a frequency of 1 HZ and an amplitude of 4 degrees about a mean angle of incidence of 15 degrees. The data indicate that under the conditions tested, there is no massive flow reversal occurring anywhere over the tip region. The velocity distributions were however highly distorted from the usual boundary layer-like shapes and exhibited significant hysteresis between the pitch-up and pitch-down parts of the oscillating cycle. There was a small but significant amount of cross-flow even at the most inboard station measured. The vicinity of the wing tip was characterized by a strong axial vortex, which originated at a distance of about 30% chord from the leading edge and grew to a size of about 20% chord at the trailing edge. The extensive set of velocity data have been archived on electronic storage and are available to any interested user.

14. SUBJECT TERMS
aerodynamics, dynamic stall, three-dimensional flows, vortex dynamics, flow measurements

15. NUMBER OF PAGES
37

16. PRICE CODE

17. SECURITY CLASSIFICATION OR REPORT	18. SECURITY CLASSIFICATION OF THIS PAGE	19. SECURITY CLASSIFICATION OF ABSTRACT	20. LIMITATION OF ABSTRACT
UNCLASSIFIED	UNCLASSIFIED	UNCLASSIFIED	UL

NSN 7540-01-280-5500

Standard Form 298 (Rev. 2-89)
Prescribed by ANSI Std. 239-18
298-102

LDA MEASUREMENTS OVER AN OSCILLATING RECTANGULAR WING

Final Progress Report

B.R. Ramaprian

March 1997

U.S. Army Research Office
Grant No. DAAH04-95-1-0170

School of Mechanical and Materials Engineering
Washington State University
Pullman, WA

TABLE OF CONTENTS

TABLE OF FIGURES

INTRODUCTION

A comprehensive experimental study has been in progress at Washington State University under ARO support during the past several years to study the vorticity dynamics and dynamic stall in the unsteady three-dimensional flow over the tip region of a rectangular wing oscillating sinusoidally in pitch about its quarter-chord axis. Under this research program, the surface pressure distributions over the stationary and oscillating wing, as well as three-dimensional boundary layer velocity measurements over the stationary wing were completed during the earlier ARO Grant periods. The results from these experiments have already been reported in the previous years. As the final phase of this program, phase-locked boundary layer velocity measurements over the oscillating wing were completed during the present ARO Grant period, namely May 1, 1995- December 31, 1996. In these experiments, fiber-optics based three-component Laser Doppler Anemometry (LDA) was used for measuring the three velocity components in the boundary layer. These measurements are extensive both in terms of the number of measurement stations over the wing surface, and the wall proximity and density of the data points at each measurement station. To the best of the PI's knowledge, these data are the first of their kind to be reported in the literature. A brief summary of the research accomplishments made during the present Grant period is given in this Final Progress Report. A more detailed description of the investigation and an extensive discussion of the data will appear in a forthcoming Ph.D. thesis and in several conference papers to be presented later during this year.

EXPERIMENTAL SET-UP AND PROCEDURE

The experiments were performed in a low-speed wind tunnel with a 0.9 m x 0.9 m (3 ft x 3 ft) test section at a freestream velocity (U_∞) of about 18 m/s (60 ft/s). Figure 1 shows a schematic of the experimental set-up and the co-ordinate system used for the presentation of data. The experimental set-up has been described in detail in earlier papers. Briefly, it consists of a NACA 0015 rectangular wing model of 0.3 m (1 ft) chord (c) and 0.6 m (2 ft) semi-span,

mounted as a cantilever from the wind tunnel side wall. A Scotch-yoke mechanism driven by a speed-regulated D.C. motor oscillates the wing sinusoidally about its quarter-chord axis. The oscillation conditions are: frequency (f) = 1 Hz (reduced frequency $k=\pi fc/U_\infty=0.05$), mean incidence ($\bar{\alpha}$) of 15 degrees and amplitude ($\Delta\alpha$) of 4 degrees. Velocity measurements (traverses in the z-direction) were made in the vertical layer over the suction side of the wing in the chordwise domain $0< x/c <1$ and spanwise domain $0<y/c <0.66$. Figure 2 shows the locations of velocity traverses. These are locations at which phase-locked surface pressure data under the same flow conditions are available from earlier experiments. At each station, data were obtained at about 40 points across the boundary layer. Most of the data points were spaced as close as 0.15 mm at x/c=0.05. The spacing was progressively increased to 1 mm at the station near the trailing edge. The density of the data obtained is adequate to enable one to estimate with acceptable accuracy the chordwise and spanwise components (ω_x, ω_y) of phase-locked vorticity distributions across the vortical layer, as well as the fluxes of these vorticity components at the wing surface.

Velocity measurements were made by using the three-component, 6-beam, 3-color, fiber optics based LDA, whose dual probes were traversed by a 3-dimensional automated traverse. The flow was seeded using latex particles of approximately 0.2 micron size injected into the plenum chamber upstream of the wind tunnel contraction through an aerodynamically profiled nozzle, using a TSI atomizer. The light scattered by the seed particles was collected off-axis by the two LDA probes and transmitted by multi-mode fibers to three photo-multipliers. The photo-multiplier outputs were processed by three counter processors. The instantaneous outputs from the three counters along with the instantaneous angle of incidence (output from the shaft encoder on the oscillating mechanism) were acquired and stored. A total of 3000 data points were collected at each probe location. These data came typically from 250-1800 oscillation cycles (collected over a period of 4-30 minutes). These were later processed to obtain the phase-locked velocity components U_x, U_y, and U_z as functions of the angle of incidence. The data from each probe location were used to reconstruct the instantaneous velocity distribution at fixed angles of

incidence during the upward (pitch-up) as well as downward motion (pitch-down) of the nose of the wing during the oscillation cycle.

It may be noted that in these experiments, the LDA probe volume remained fixed in wind tunnel co-ordinates, as the wing surface moved up and down during the oscillation cycle, often crossing the probe volume (when the probe volume was in the inner part of the vortical layer). The strong reflection of light by the wing surface during these crossings caused serious difficulties in the data acquisition process. After several months of trial, this problem was finally overcome by designing the instrumentation and data acquisition procedure such that wing surface crossings could be detected. The LDA counters would then be automatically stopped from collecting data during the unwanted period. A schematic of the instrumentation used is shown in Fig.3.

Velocity data were obtained at about 60 locations over the wing. Only some typical results and important observations are presented in this Report. The complete set of data along with detailed analysis and discussion of the results will be provided in the forthcoming thesis of J. Szafruga. Also, the data have been archived on magnetic storage and are available to any interested user.

Data for the pitch-up and pitch-down motions were ensemble averaged separately. Each data point shown in the figures in this Report generally represents an ensemble average of 20-200 samples. The number of samples obtained in each case depends on various factors such as the measurement station, the incidence angle, the part of the oscillation cycle (i.e. pitch-up or pitch-down) and on the average distance of the probe volume to the surface during the oscillation cycle. Furthermore, the data presented in this Report have been averaged over an incidence window interval of about ±0.1 degree (corresponding to ±5 encoder steps). The archived data can be reprocessed using any other window interval if desired. The sample size would vary depending on the choice of this interval. With the data processing parameters selected, the following are the estimated uncertainties in the measurements: location of the probe volume (x,y,z); 0.05 mm, U_x; 1%, U_y; 5%, U_z; 3%. Apart from the above, the spatial and temporal (angular) resolutions associated with ensemble averaging are separately discussed later.

RESULTS

Velocity Distributions

Figures 4 and 5 show the variation of the phase-locked velocity components as a function of the incidence angle at two end stations (x/c= 0.05; y/c=0.66 and x/c=0.95; y/c=0.03) diagonally opposite from each other. At each station, data are shown for three fixed z/c-locations inside the vortical layer. These locations are indicated in Figs.6 and 9 and identified by their file numbers. Data for the pitch-up motion are shown by filled symbols and the data for the pitch-down motion are shown by the open symbols. The following points can be observed from Figs.4 and 5.

1. There is hysteresis in the velocity field between pitch-up and pitch down in many cases, as indicated by the loops. The loops may run clockwise (pitch-up velocities being larger than pitch-down velocities), counterclockwise, or may form the figure of 8. The behavior may also change from the edge of the boundary layer towards the wing surface.
2. The cross-flow in the tip-region is quite strong (V of the order of U_∞).
3. In general, there is larger scatter in the data during the pitch-down motion, especially at the in-board location. This is possibly due to the occurrence of some flow separation (in the more downstream part of the wing) at the beginning of the pitch-down motion. Some scatter observed in the data in the outboard station is primarily due to the unsteadiness associated with the tip vortex formation.
4. The data from locations **51** and **45** (files s9503**051** and s0566**045**) corresponding to "lower" positions in the vortical layer clearly show the crossing of the measurement location by the wing surface during its oscillation. Since the two locations are on opposite sides of the pitching axis, the interference at these locations occurs at the lower (< 13.5 deg) and upper (>16 deg) ends respectively, of the oscillation cycle. Thus, location **51** remains below the wing surface at incidences lower than about 13.5 deg, while location **45** remains below the wing surface at higher than about 16-deg incidence.

Figures 6-9 show the instantaneous velocity distributions across the vortical layer at stations located at the four corners of the wing surface region studied. Figures 6 and 7 show the results for the upstream stations (x/c=0.05) at the two spanwise locations (y/c=0.66, and y/c=0.03). Figures 8 and 9 show results for the same spanwise locations near the trailing edge (x/c=0.95). In each case, the distributions of all the three velocity components U, V, and W are shown for three instantaneous incidences α=12, 15, 18 degrees. Once again, results for pitch-up and pitch-down motions are identified by filled and open symbols respectively. As already stated, an averaging window of 0.2 degree is used in all cases. The resulting spatial resolution (i.e. the distance over which the velocity is averaged), which is proportional to the distance of the location from the pitching axis, is approximately equal to 0.2 mm (0.0007c) and 0.7 mm (0.0025c), at the upstream and downstream locations respectively. In each of the figures, the instantaneous position of the oscillating wing surface is shown by the vertical dashed line. The distance of the data point closest to the surface is less than 0.2 mm for the upstream stations and less than 0.7 mm for the downstream stations. They are thus within the spatial resolution of the measurement scheme.

The following are the observations that can be made from Figs. 6-9.

1. The viscous boundary layer thickness at x/c=0.05 (Figs.6 and 7) is generally about 1 or 2 mm at both the spanwise locations, and is barely measurable, especially at the smaller incidences. The decrease in U in the region beyond the viscous boundary layer at the lower incidences is due to the convex curvature of the streamlines.
2. The cross-flow velocity was seen to be very small at all the inboard locations. This is borne out in particular, by the data shown in Figs.7. The cross-flow data at the upstream inboard station in Fig.6 (measured early in the Program) appears to be very noisy and not very reliable. The data obtained subsequently at other stations were more reliable as an improvement was incorporated in the optical configuration of the LDA.
3. The vortical layer thickness at the in-board downstream station (Fig.8) varies from about 5% of chord at 12 degrees incidence to more than twice that value at 18 degrees incidence. The shape of the velocity distribution also changes significantly during this oscillation interval.

The velocity distribution at 18 degrees shows a region of flat distribution or zero vorticity near the wall. No reversals in the phase-locked velocity component U are observed, even though small negative values were observed in some of the instantaneous data in the ensemble. It is reasonable to conclude that no massive separation occurred in the flow. It is interesting that the pitch-up and pitch-down data for U coincide fairly well at 18-degree incidence but exhibit significant divergence at the lower incidences. This is due to the time lag in the response of the flow to the varying incidence. It is also important to note that there is a small amount of cross-flow at this inboard location, mostly very near the wall.

The velocity distributions shown for the downstream tip region in Fig.9 clearly show the presence of the tip vortex. Here, the cross-flow velocity attains magnitudes comparable to the freestream velocity and exhibits the S-shaped profiles characteristic of three-dimensional boundary layers experiencing shear-layer lift-off (as in the case of boundary layers over bodies of revolution at incidence). The velocity variations extend over a region as wide as $0.15c$- $0.2c$. This region is dominated by the tip vortex. It may be possible to recognize from the U-distribution, a thin "boundary layer" of a few mm thickness, submerged underneath the vortex. Outside this region, the U-profile exhibits a minimum at the vortex center, which is consistent with the observations made from the tip vortex measurements made by us some years ago in the wake downstream. However, in the earlier experiments, the angle of incidence varied between 5 and 15 degrees, compared to the incidence range of 11-19 degrees in the present experiments. The velocity maximum seen in the outer part of the vortical layer in the present data was not observed in the earlier measurements.

Velocity vectors

A global visualization of the spatial and temporal structure of the three-dimensional velocity field over the oscillating wing is provided by the series of vector plots shown Figs.10-21. These show some typical examples of the phase-locked velocity vectors in streamwise and spanwise planes. These include the two extreme streamwise planes y/c=0.66; y/c=0.03 and the two cross-stream planes x/c=0.29; x/c=0.95. In each case, results are shown for three incidences,

α= 12, 15 and 18 deg respectively, and separately for pitch-up (α increasing) and pitch-down (α decreasing). In all the figures, the data are shown without performing any smoothing or interpolation. The figures show that within practical limits, the measurements have covered all the important regions of the flow. The instantaneous position of the oscillating wing surface is shown in Figs. 10-15. The instantaneous position of the local wing surface and that of the trailing edge are shown in Figs.16-21.

Referring first to the results for the in-board plane y/c=0.66 in Figs.10-12, it can be seen that the vortical layer in this plane extends up to about 0.15c from the wing surface during the oscillation cycle. It is also seen that the velocity distributions begin to develop "unusual" non-boundary-layer-like shapes from about x/c=0.4 onwards even at a low angle of incidence of 12 degrees during pitch-up. These trends continue as the angle of incidence increases. In particular, a layer of flat velocity distribution (or zero velocity gradient) develops next to the wall at the higher incidences. This region continuously grows in extent as the incidence increases and extends as far upstream as x/c=0.3 at the highest incidence shown. The distributions during pitch-down are, with a few exceptions, significantly different form the above. Also, they exhibit greater scatter and more flow structures. The differences between pitch-up and pitch-down were observed to be, in general, the most pronounced at the mid-incidences, as to be expected. This is also seen from the above figures. Finally, it is clear from Figs.10-12 that there is no upstream flow in this plane in the oscillation interval shown.

Figures 13-15 show the velocity field in the plane y/c=0.03 which is close to the wing tip. First of all, it is seen that there are a few regions in the flow where the velocity data are missing. This is because no valid data could be obtained in those regions. This was either due to the absence of the seed particles or due to insufficient number of data samples. These data "holes" were observed only in some runs, and when observed, were generally found to coincide with the vortex locations. It is not clear whether the seed particles were centrifuged out by the vortex in these cases, or whether these regions were not along the trajectory of the injected seed particles.

It is seen however, that these "holes" in the data are not extensive and have not resulted in any significant loss of information.

The velocity distributions in this streamwise plane are very nearly flat, except for some slight undulations. They are thus essentially "featureless" especially in comparison with those in the in-board plane, and by themselves, give no clue to the presence of a vortex. They, in fact, lead one to conclude that the "boundary layer" next to the surface is, for the most part, very thin. There is also no significant difference between velocity distributions during pitch-up and pitch-down motions. There is also no evidence of any flow reversals in the streamwise plane and no indication of severe adverse pressure gradients that are usually precursors of stall.

Figures 16-18 show the velocity vectors in the cross-stream plane at the upstream position x/c=0.29. The velocity variations are seen to extend up to and even beyond 0.15c in the region close to the tip. Since the vectors have been drawn to the *same* scale in Figs.10-21, one can study the magnitude of the cross-flow in comparison with the streamwise flow. First, it can be seen that the cross-flow quickly decreases towards in-board and is very small at the most-inboard plane of measurement y/c=0.66 at all angles of incidence during both pitch-up and pitch-down motions. At 12-degree incidence, the wing tip vortex has not formed yet during the pitch-up motion and has apparently been destroyed during the pitch-down motion. Beginnings of the vortex are barely noticeable near the tip and very near the surface at 18-degrees incidence. The vortex can be assumed to originate in the vicinity of this x-location, with the origin translating over a small distance upstream and downstream as the angle of incidence increases and decreases.

Finally, Figs.19-21 show the cross-stream flow field near the trailing edge (x/c=0.95). Here, a strong vortex can be seen at all incidences during both pitch-up and pitch-down motions of the wing. The tangential velocities within the vortex are as large as the free-stream velocity. The velocity variations extend well beyond 0.25c from the surface. Cross-flow velocities are still somewhat significant at the most inboard station x/c=0.66. With reference to the instantaneous position of the local wing surface, the vortex has been lifted off by about 0.05c from the surface at the 12-degree incidence, and by about 0.15c at the 18-degree incidence. A careful observation

will show that there is a slight difference in the vortex location between pitch-up and pitch-down motions. While there exist some hysteresis effects, these are not very strong in the tip region. It is also interesting to note that in the spatially fixed co-ordinate system chosen, the vortex height does not vary much during the oscillation of the wing.

Figure 22 shows a repeat plot of Fig.21, but with lines drawn parallel to the velocity vectors in the cross-stream plane. These lines can also be regarded as the projection of the instantaneous streamlines in the cross-stream plane. They show some of the topological features associated with the flow in the wing tip region. In particular, the "eye" of the tip vortex and the line AB separating the vortex from the rest of the flow can be seen clearly. Fluid particles originating in the tip region below AB will be trapped in the vortex while those originating above AB will move inboard. Their flow paths in the cross-stream plane are modulated during the oscillation of the wing. It is seen that there is a significant downward component of the velocity in the inboard region, showing that the flow does not leave the surface and "separate" in the steady, two-dimensional sense. This explains the observation of very mild dynamic stall experienced by the flow under the present oscillating conditions, even in the most in-board station measured.

CONCLUSIONS

A very extensive set of phase-locked velocity data have been obtained in the three-dimensional flow over the tip region ($y/c<0.7$) of the oscillating wing. These data clearly indicate that under the oscillation conditions studied, while there is significant hysteresis in the flow field between the pitch-up and pitch-down phases of the oscillation, there is no massive stall even in the most in-board plane of measurement, namely $x/c=0.66$. In fact, very little instantaneous reversal of streamwise flow was observed in this plane. The vortical layer velocity distributions are, however, very different from conventional boundary layer distributions. The cross-flow velocities at the most inboard section studied, namely, $x/c=0.66$ are small but still significant enough, in the author's opinion, to have prevented the occurrence of strong dynamic stall.

Strong cross-flows of magnitudes comparable to the free-stream velocity characterize the flow in regions closer to the wing tip. These large cross-flow velocities are, however, confined to the immediate vicinity of the tip vortex. In this region, there is no evidence of stall, even though some hysteresis can be observed in the position and structure of the tip vortex between the pitch-up and pitch-down portions of the wing oscillation cycle.

The data obtained in the present study are very extensive and need to be processed further to obtain additional important information on the phase-locked properties of flow. These include vorticity, the direction and magnitudes of the surface shear stress (and hence the topological features of the flow at the surface), and the vorticity fluxes. This work is under progress and the results will be reported in the forthcoming Ph.D. thesis of J. Szafruga.

All the data have been archived on a set of three zip disks, each of 100 MB capacity. The disks also contain an executable program (that runs on a PC with a 486/Pentium processor) and an input file that allows the user to specify her/his data processing options (such as stations to be processed, incidence(s) required, ensemble averaging window width, etc.). The Program produces ASCII tables of data containing the phase-locked distributions, for the selected angle of incidence, of the three components of the velocity U, V, W with distance z from the wing surface. Data are tabulated separately for the pitch-up and pitch-down motions. The archived data on the zip disks can be obtained by contacting the PI. The user needs to have a PC equipped with a zip drive to use the data archival.

PERSONNEL, PUBLICATIONS AND DEGREES AWARDED

Personnel:

B.R. Ramaprian	PI
J. Szafruga	Graduate Research Assistant
	Ph.D. Degree expected in June 1997.

Publications

Szafruga, J., and Ramaprian, B.R., "LDA Measurements Over the Tip Region of a Rectangular Wing," AIAA Paper No. 95-1780.

Szafruga, J. and Ramaprian, B.R., "LDA Measurements in the Three-Dimensional Flow Over an Oscillating Wing," AIAA Paper No. 97-1935, (To be presented at the 28th AIAA Fluid Dynamics Conference, Snowmass, CO, June 29-July 2, 1997).

Szafruga, J., and Ramaprian, B.R., "Study of the Three-Dimensional Flow Over an Oscillating Wing using LDV," submitted to the AGARD 81st Fluid Dynamics Panel Symposium on Advanced Aerodynamic Measurement Technologies, Seattle, WA, September 22-25, 1997.

Szafruga, J., and Ramaprian, B.R., "Velocity measurements in the three-dimensional unsteady boundary layer over the tip region of an oscillating rectangular wing," The Seventh Asian Congress of Fluid mechanics, Indian Institute of Technology, Chennai, India, December 8-12, 1997.

Reportable Inventions

Nil

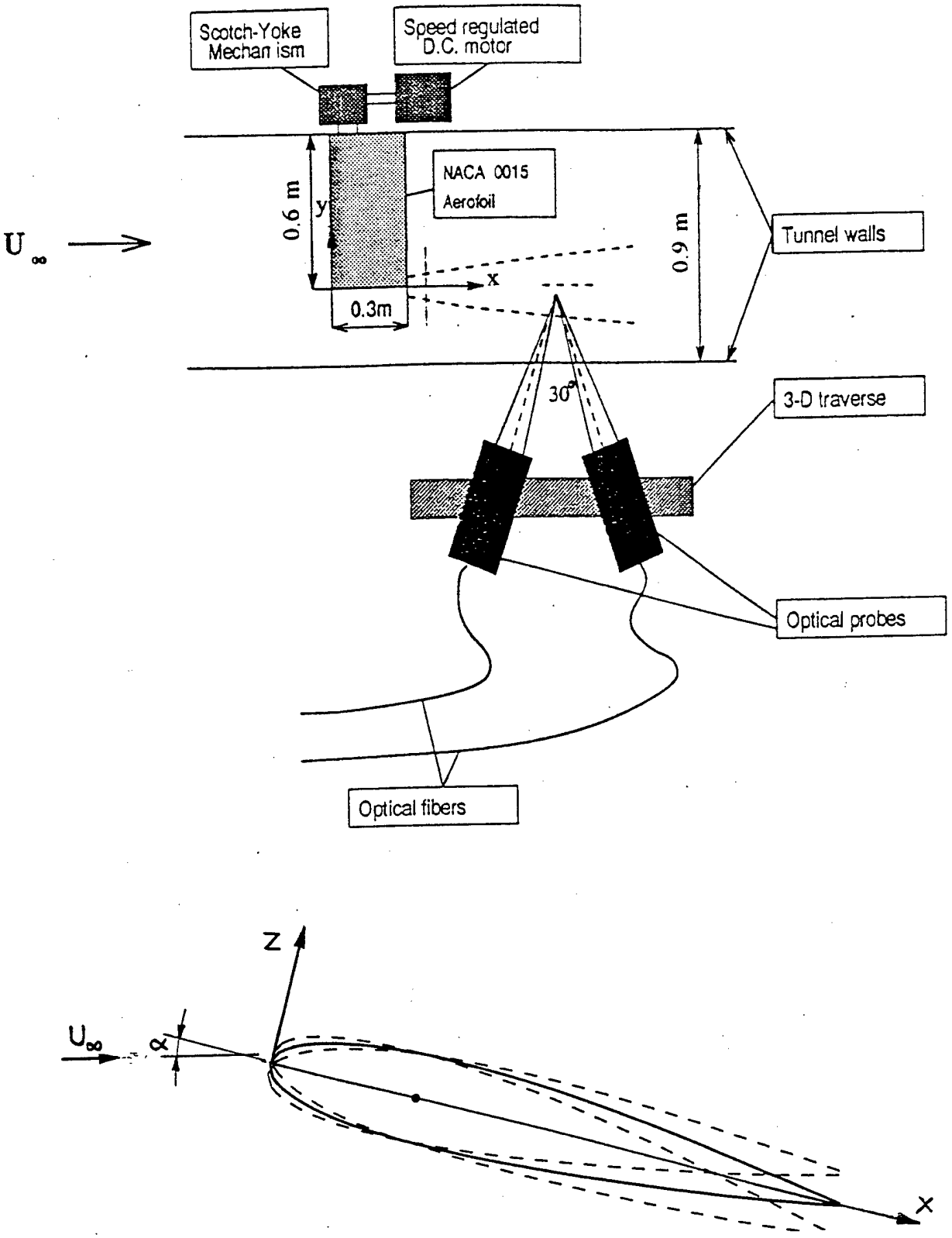

Fig.1. The Experimental set-up and co-ordinate system used.

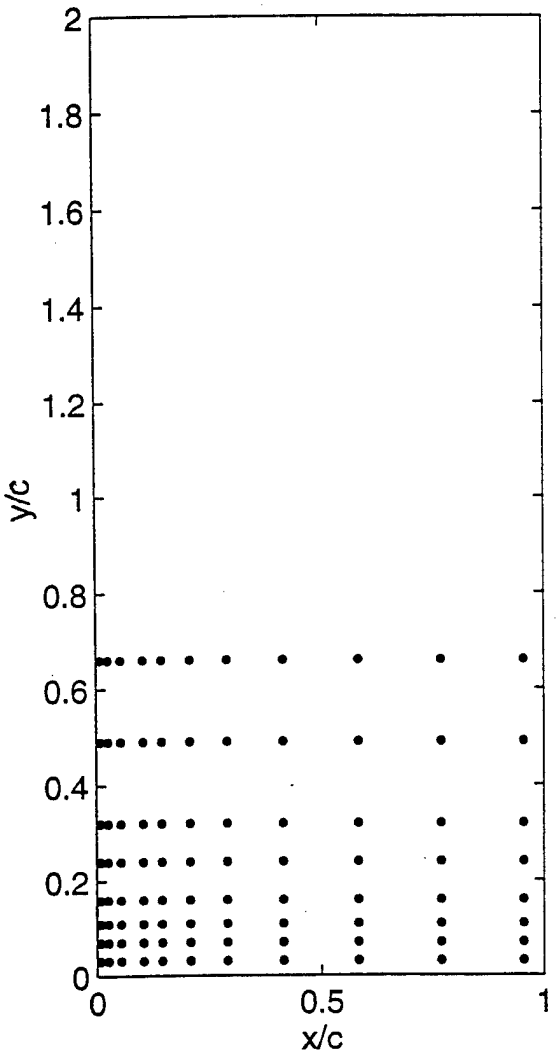

Figure 2 Location of the measurement stations on the wing surface.

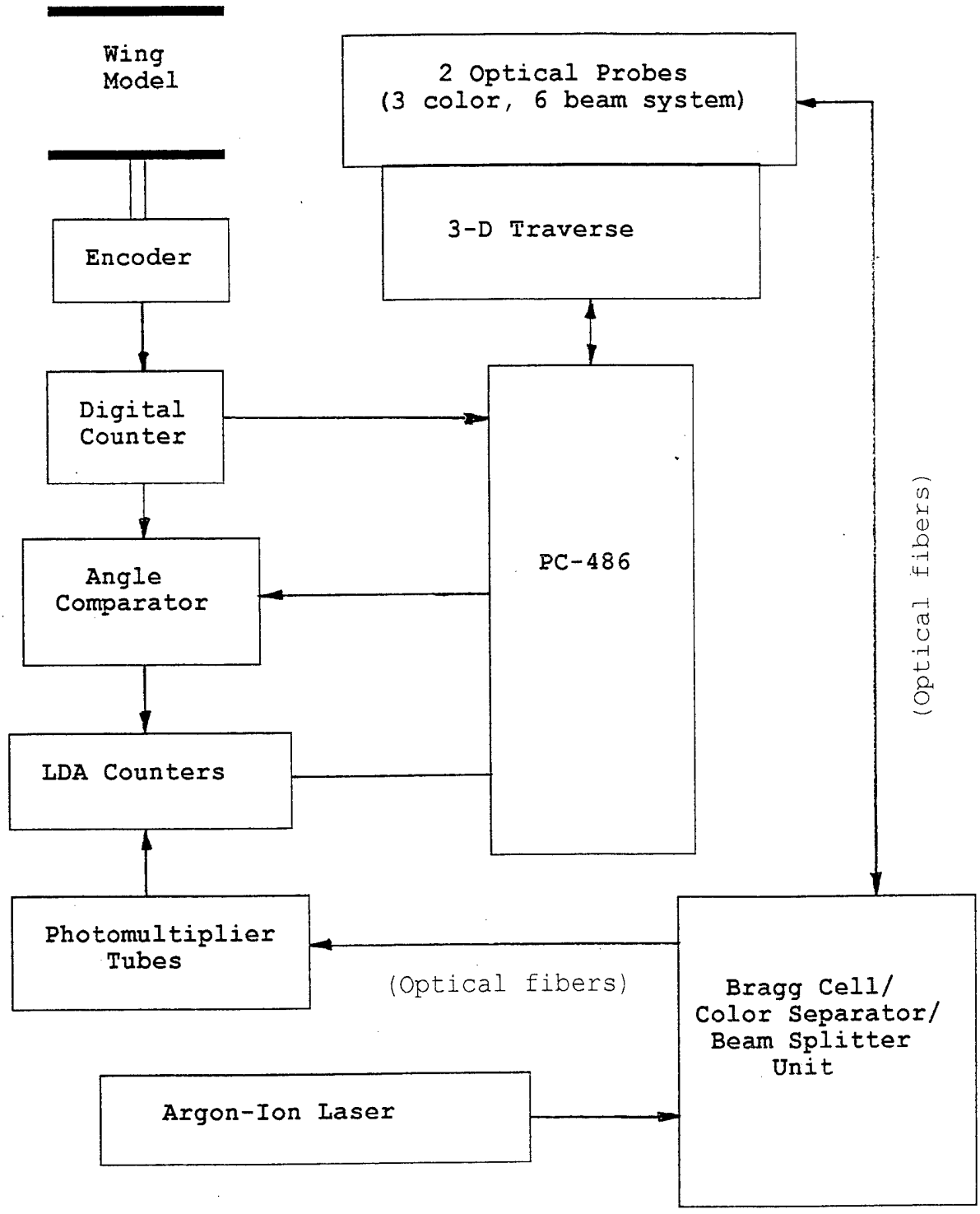

Fig. 3 Schematic of the instrumentation system used for the measurements.

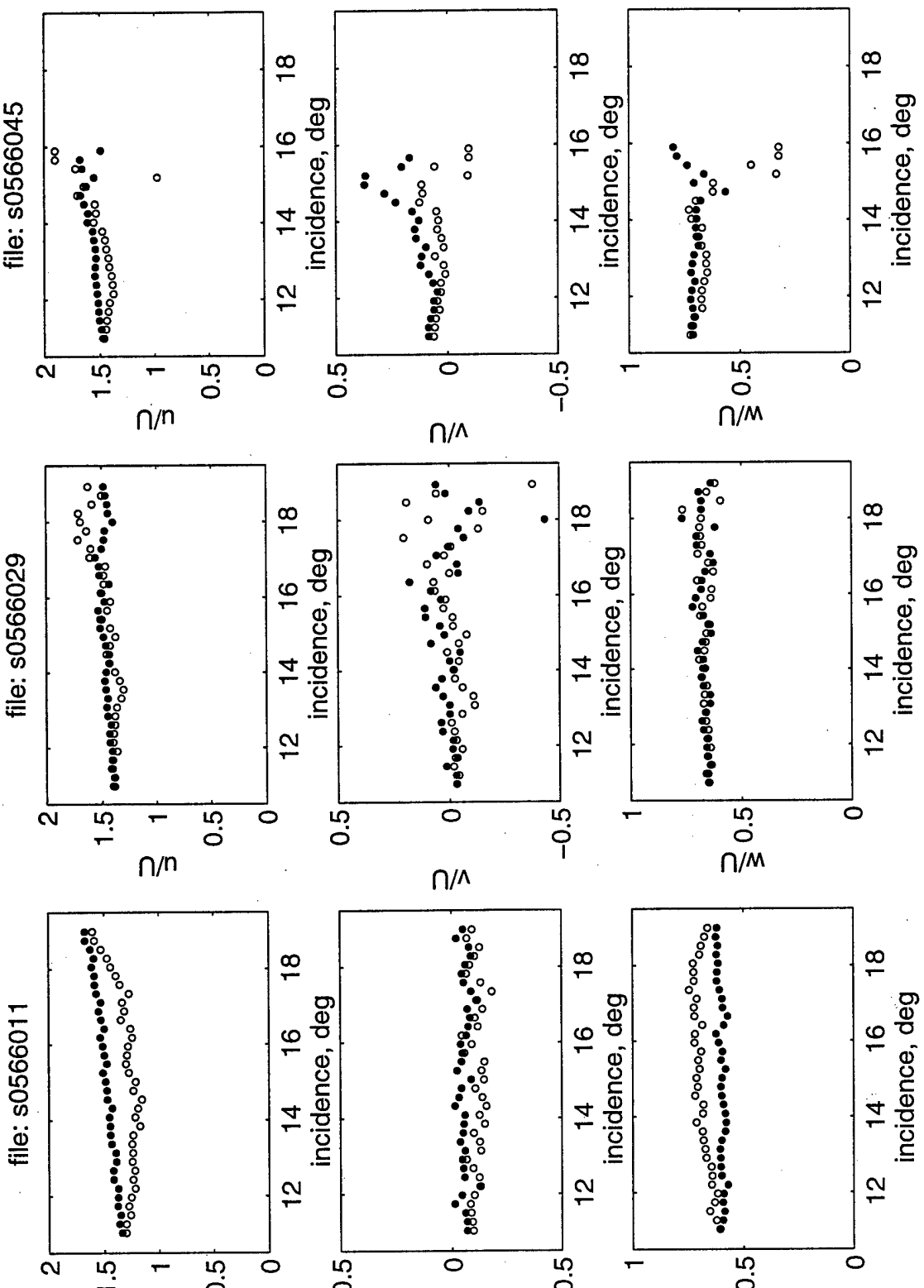

Fig.4. Variation of the phase-locked velocity components at fixed probe location, during the oscillation cycle. x/c=0.05, y/c=0.66. Probe locations are indicated by the corresponding file numbers in Fig.6. Filled symbols: pitch-up; open symbols: pitch-down.

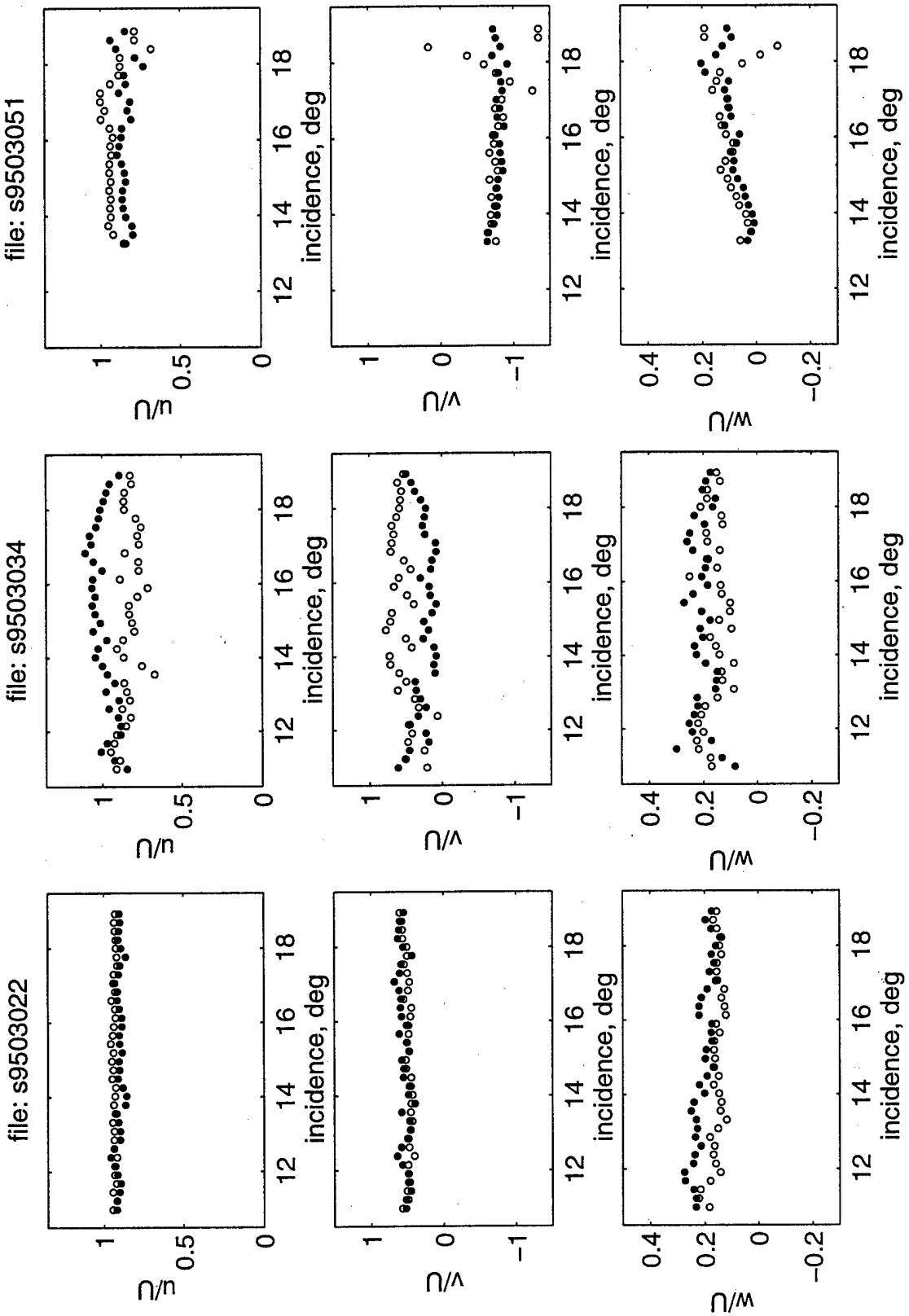

Fig. 5 Variation of the phase-locked velocity components at fixed probe location, during the oscillation cycle. x/c=0.95, y/c=0.03. Probe locations are indicated by the corresponding file numbers in Fig. 9 Filled symbols: pitch-up; open symbols: pitch-down.

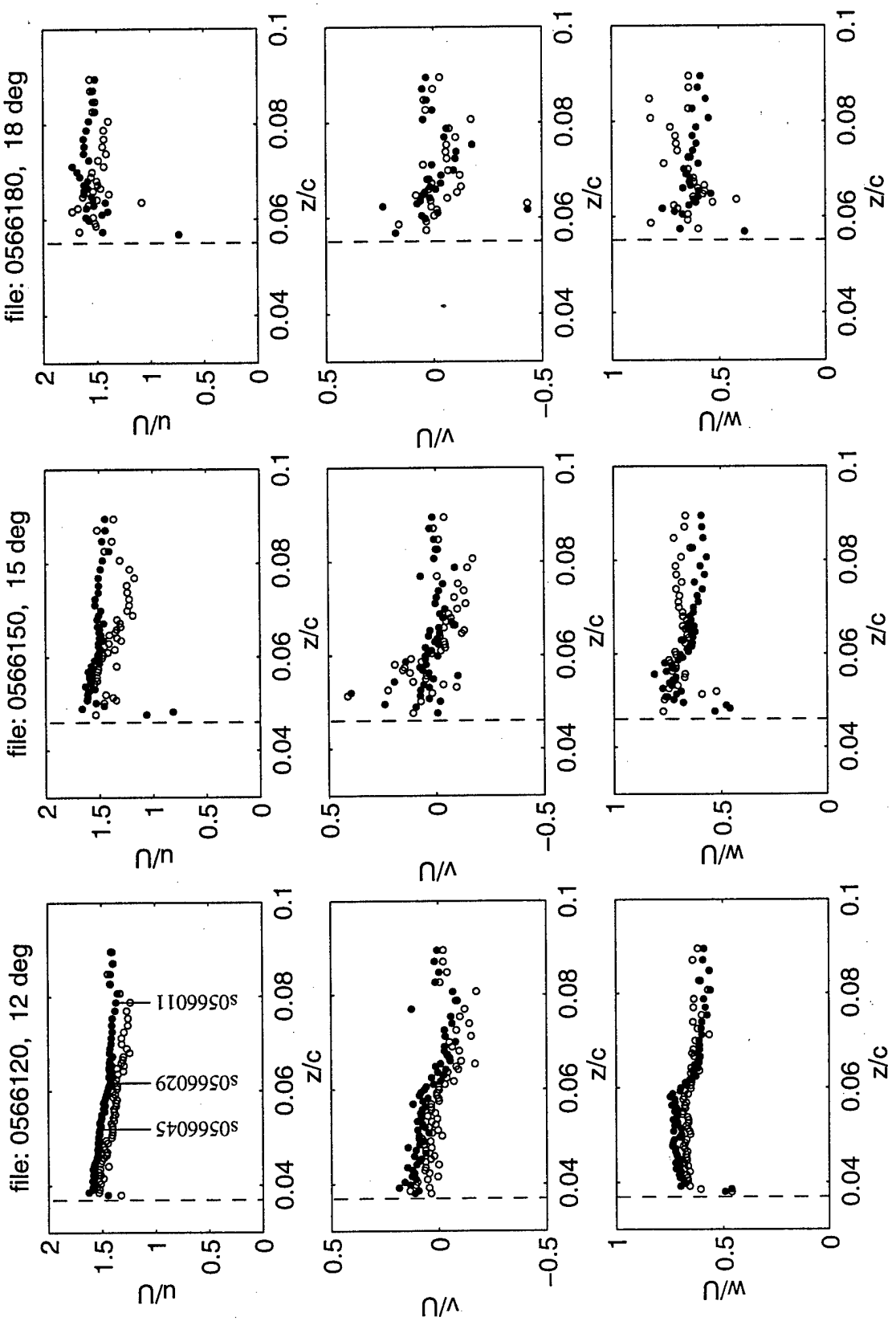

Fig.6 Velocity distributions in the vortical layer over the wing surface. x/c=0.05; y/c=0.66. The vertical dashed line in each plot denotes the instantaneous position of the wing surface. Filled symbols: pitch-up; open symbols: pitch-down.

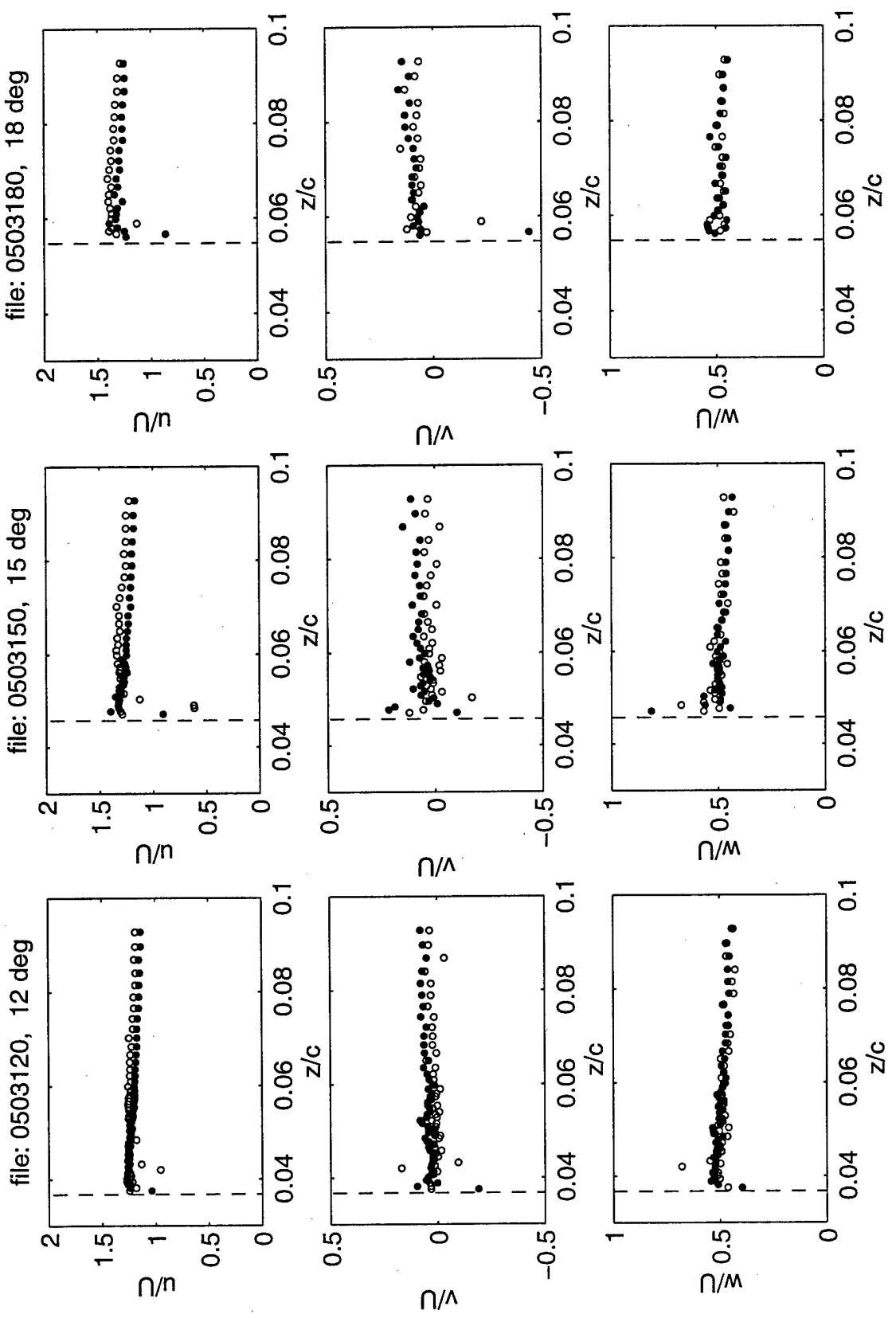

Fig.7 Velocity distributions in the vortical layer over the wing surface. x/c=0.05; y/c=0.0.03. The vertical dashed line in each plot denotes the instantaneous position of the wing surface. Filled symbols: pitch-up; open symbols: pitch-down.

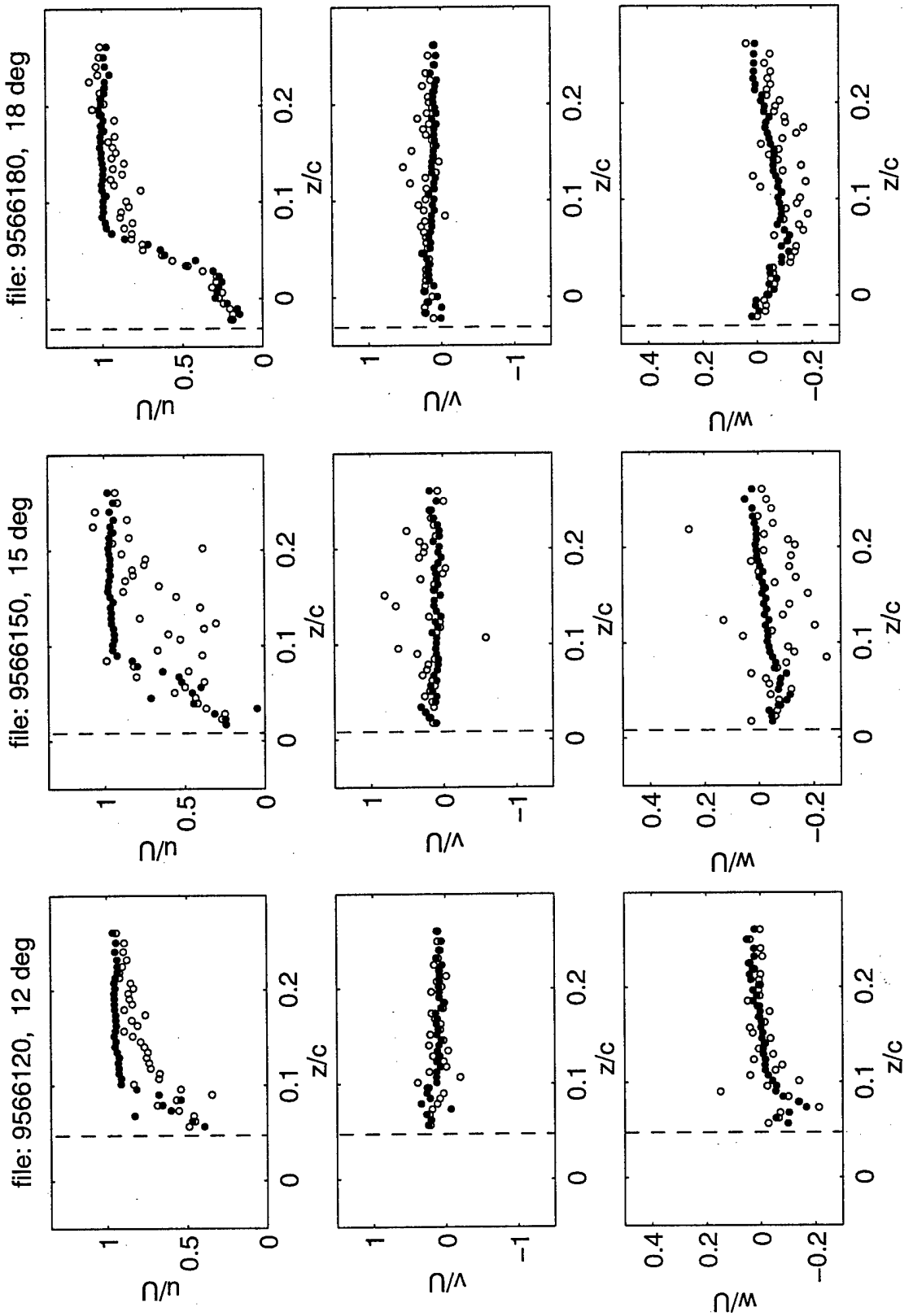

Fig.8 Velocity distributions in the vortical layer over the wing surface. x/c=0.95; y/c=0.66. The vertical dashed line in each plot denotes the instantaneous position of the wing surface. Filled symbols: pitch-up; open symbols: pitch-down.

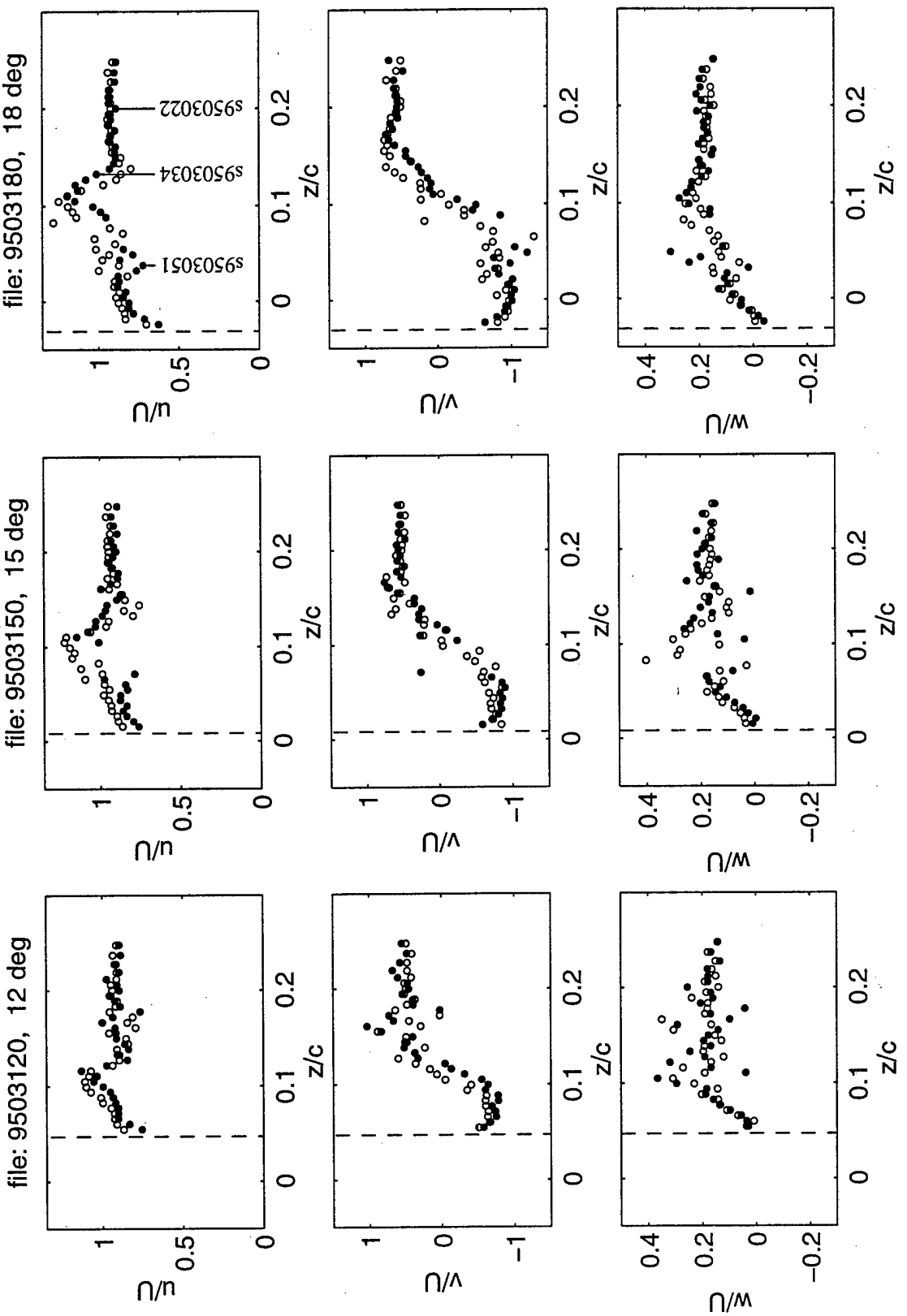

Fig.9 Velocity distributions in the vortical layer over the wing surface. x/c=0.95; y/c=0.03. The vertical dashed line in each plot denotes the instantaneous position of the wing surface. Filled symbols: pitch-up; open symbols: pitch-down.

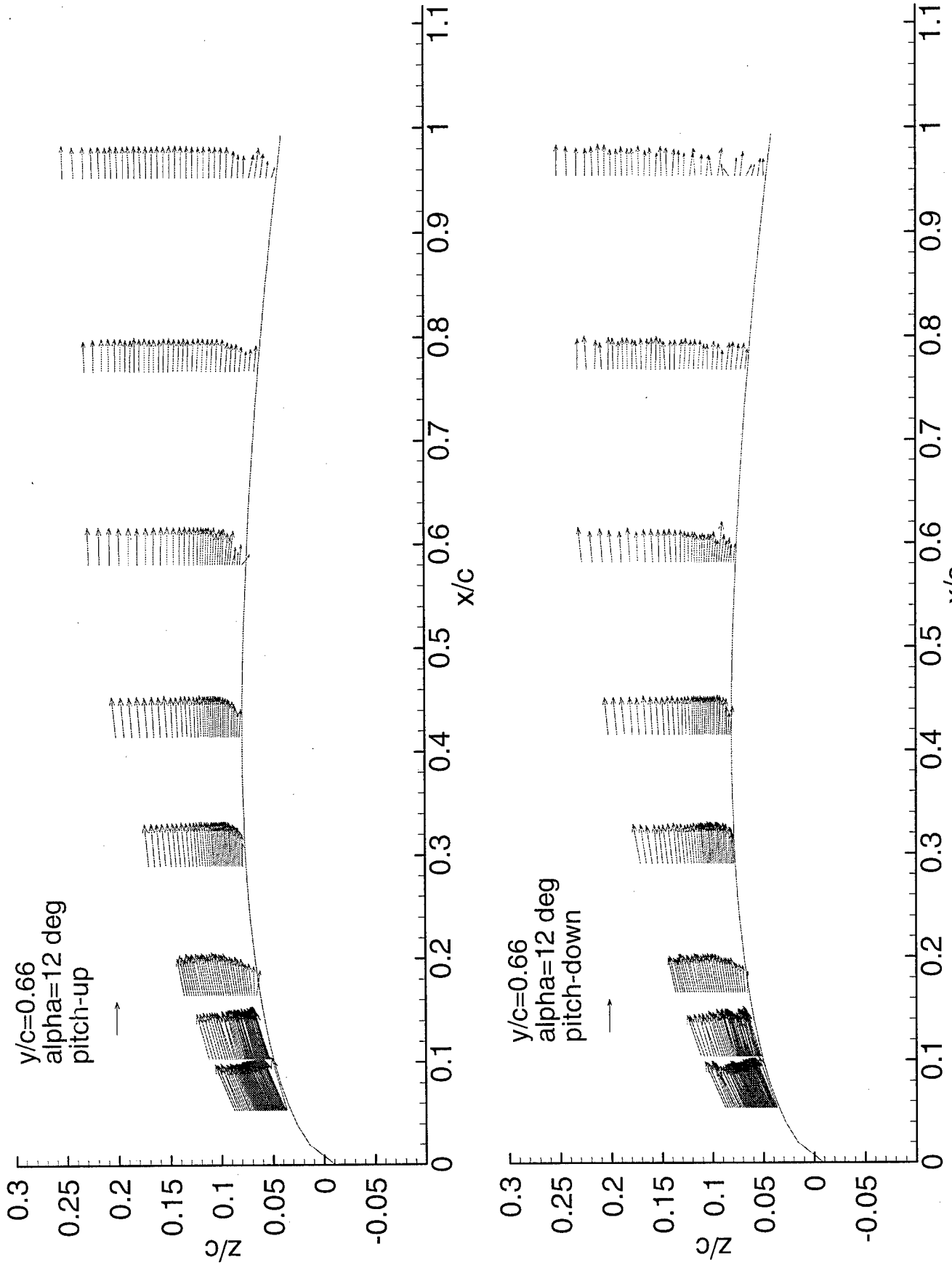

Fig.10 Velocity vectors in the in-board streamwise plane, y/c=0.66. The reference vector shows magnitude of freestream velocity.

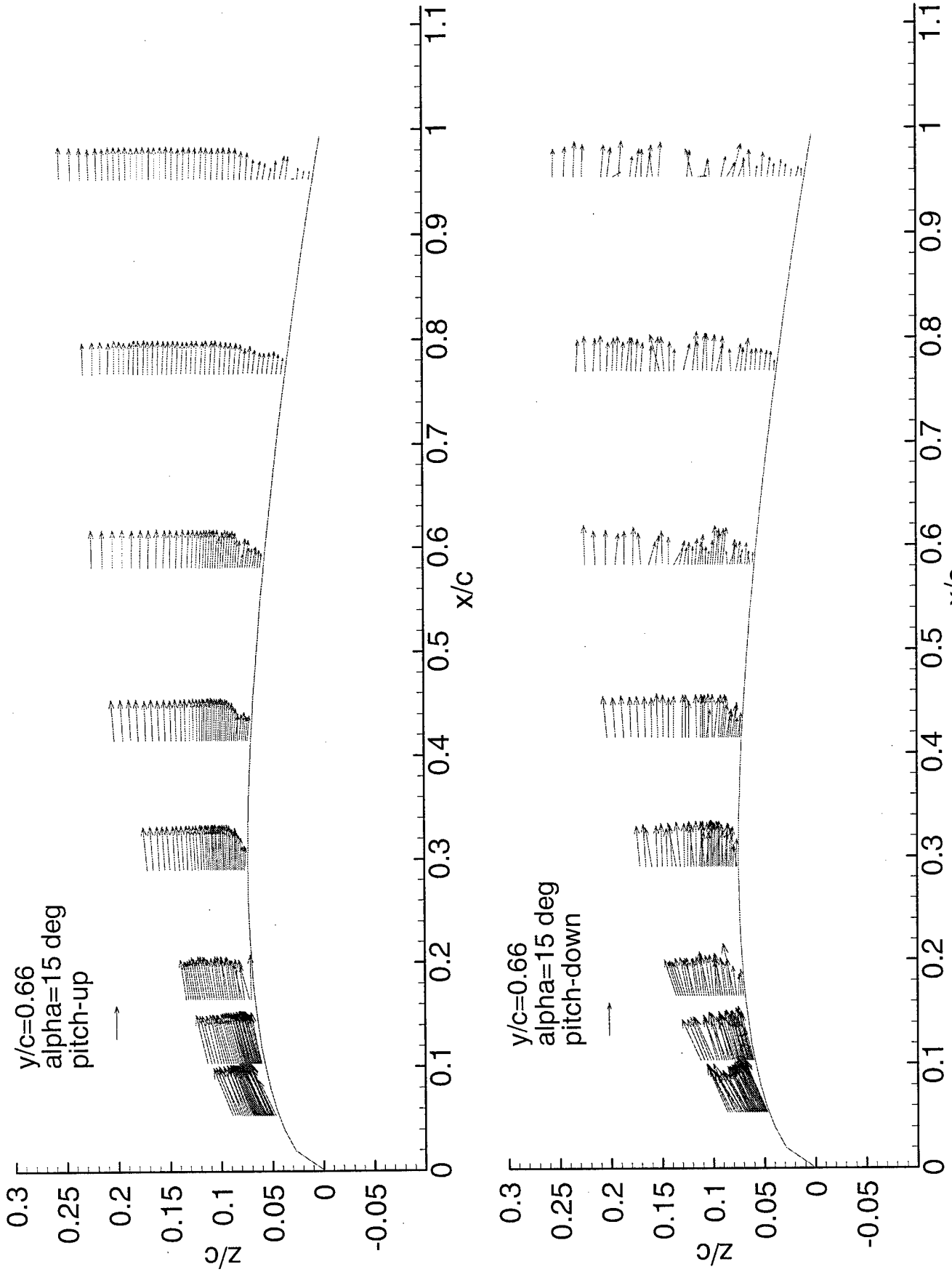

Fig.11 Velocity vectors in the in-board streamwise plane, y/c=0.66. The reference vector shows magnitude of freestream velocity.

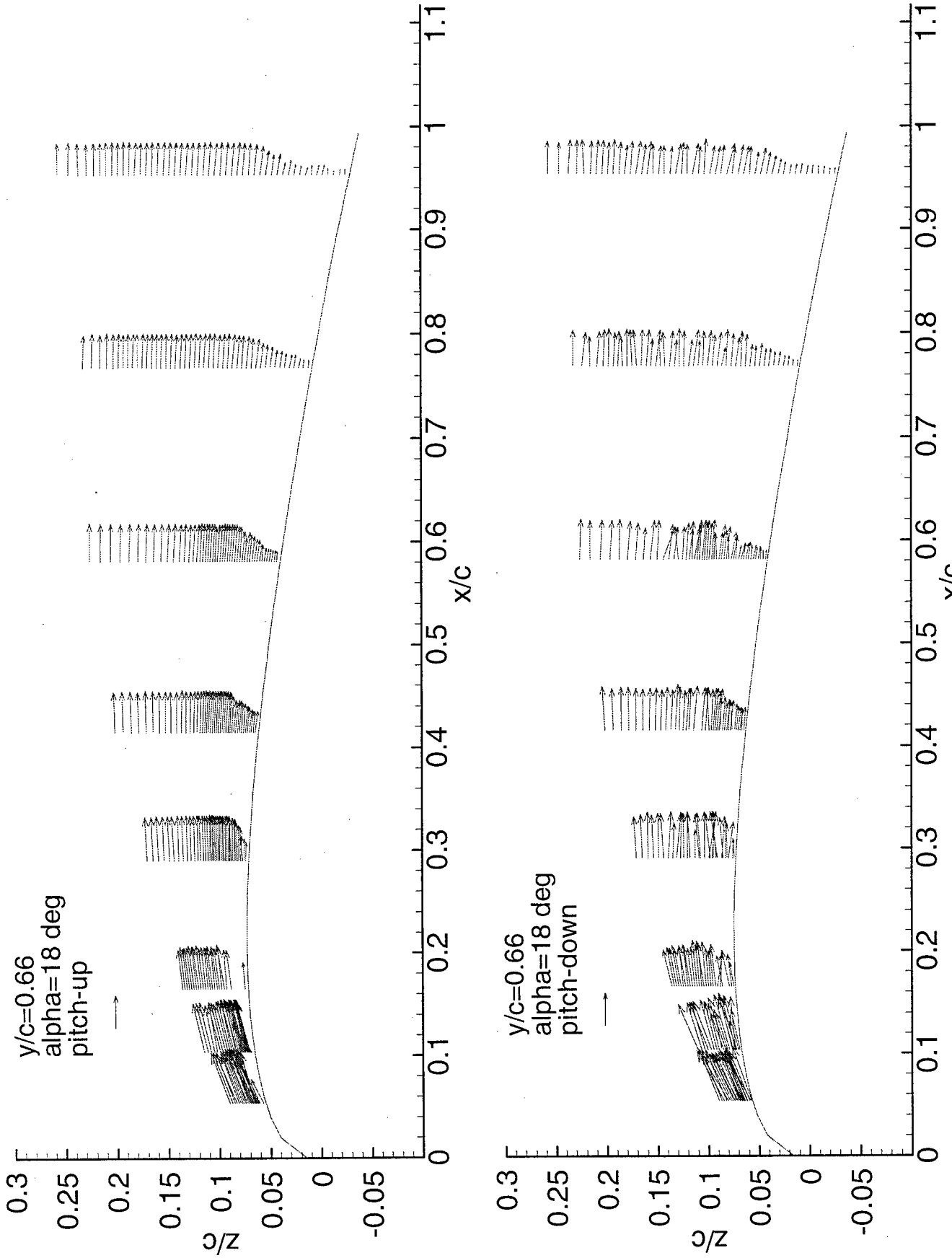

Fig.12 Velocity vectors in the in-board streamwise plane, y/c=0.66. The reference vector shows magnitude of freestream velocity.

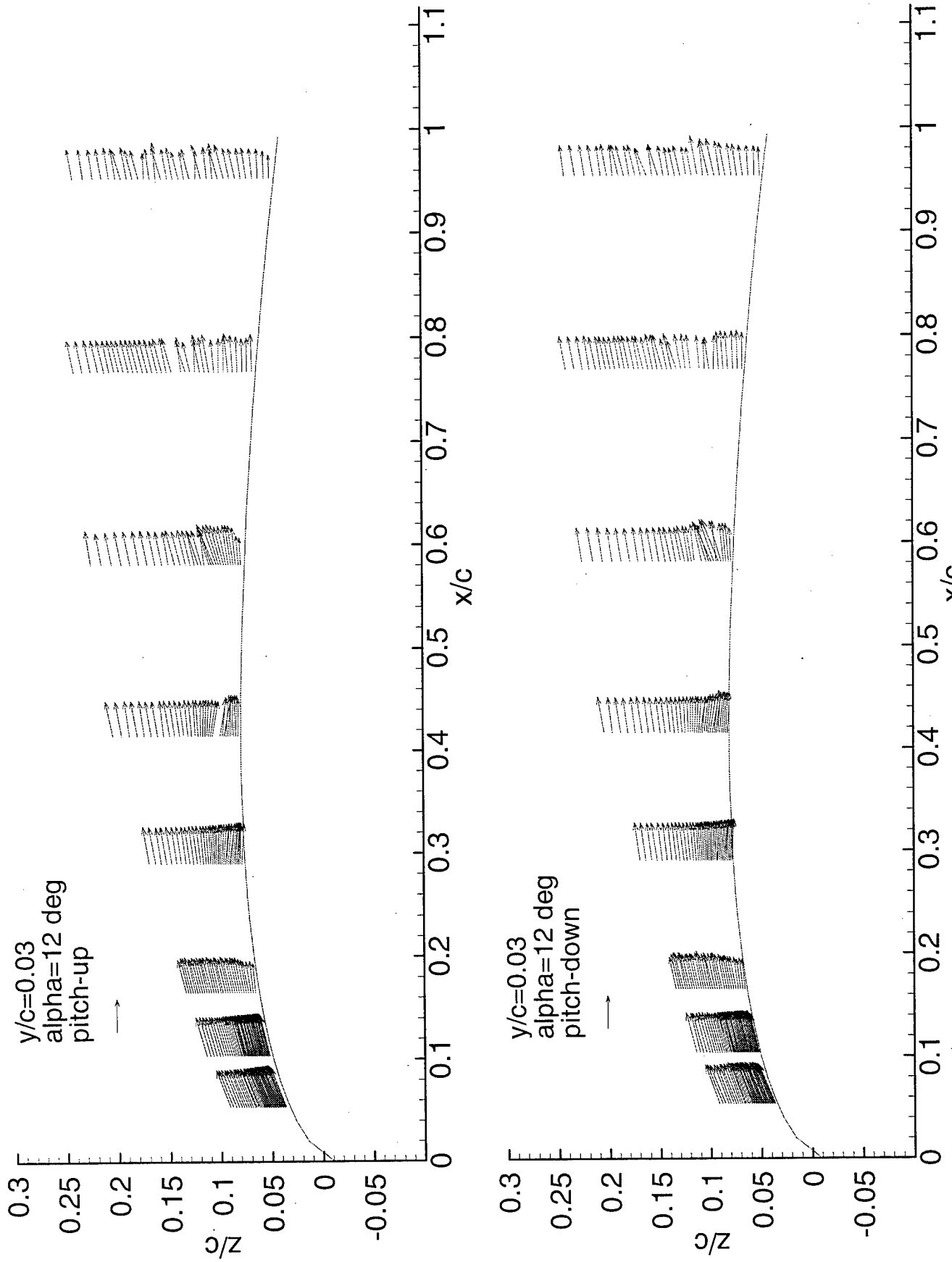

Fig.13 Velocity vectors in the streamwise plane, y/c=0.03 near the tip. The reference vector shows magnitude of freestream velocity.

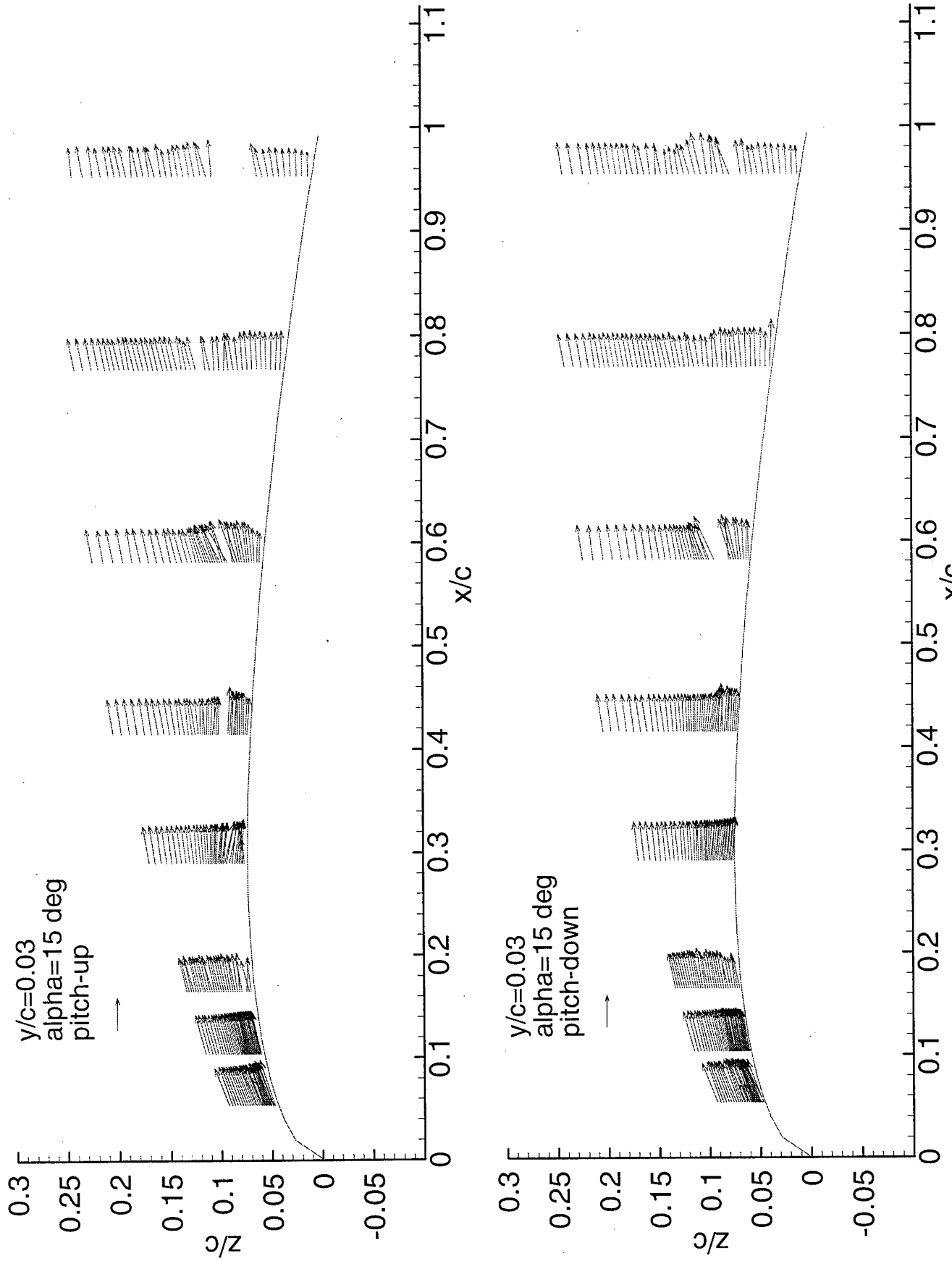

Fig.14 Velocity vectors in the streamwise plane, y/c=0.03 near the tip. The reference vector shows magnitude of freestream velocity.

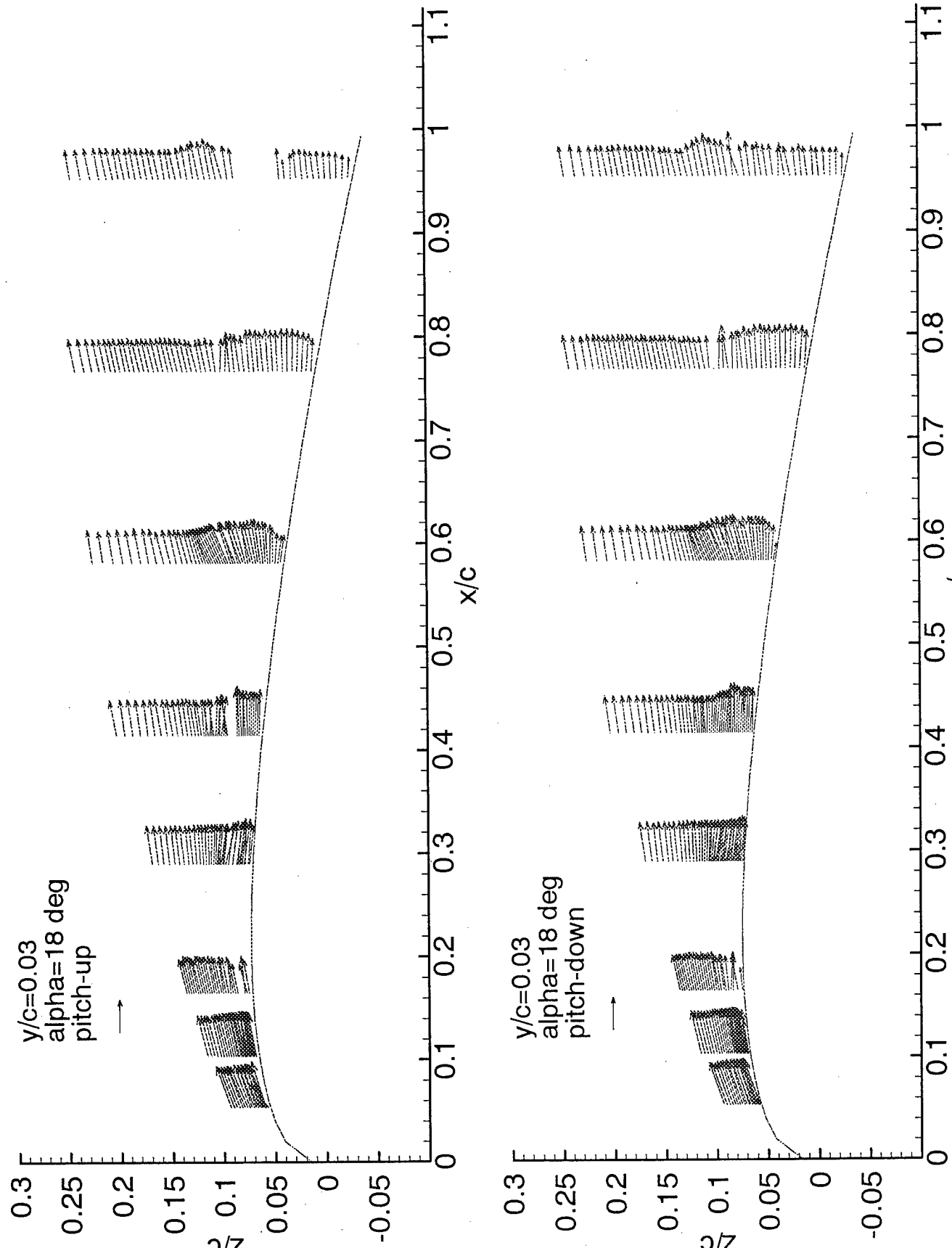

Fig.15 Velocity vectors in the streamwise plane, y/c=0.03 near the tip. The reference vector shows magnitude of freestream velocity.

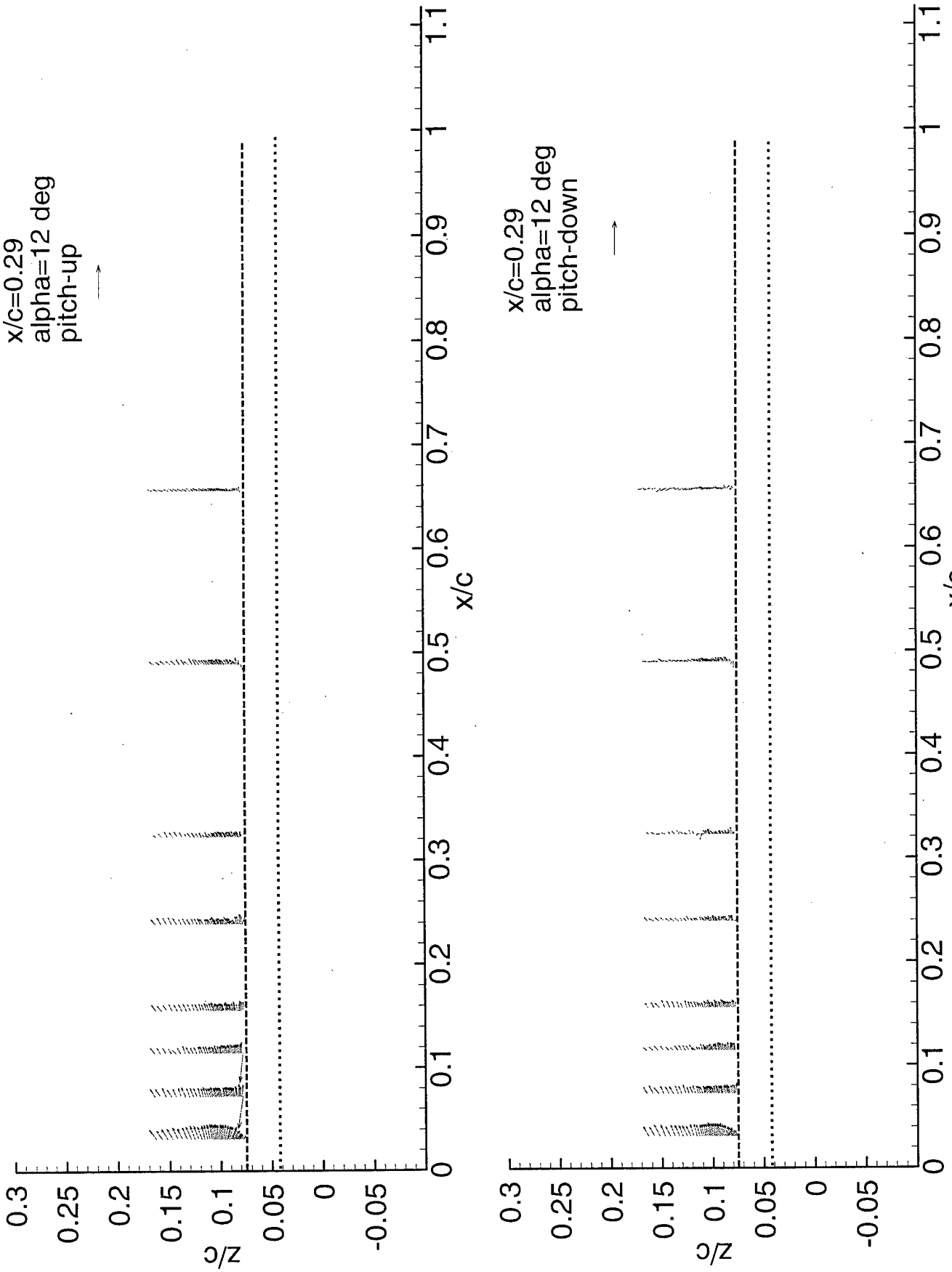

Fig.16 Velocity vectors in the cross-stream plane at x/c=0.29. The reference vector shows magnitude of freestream velocity.

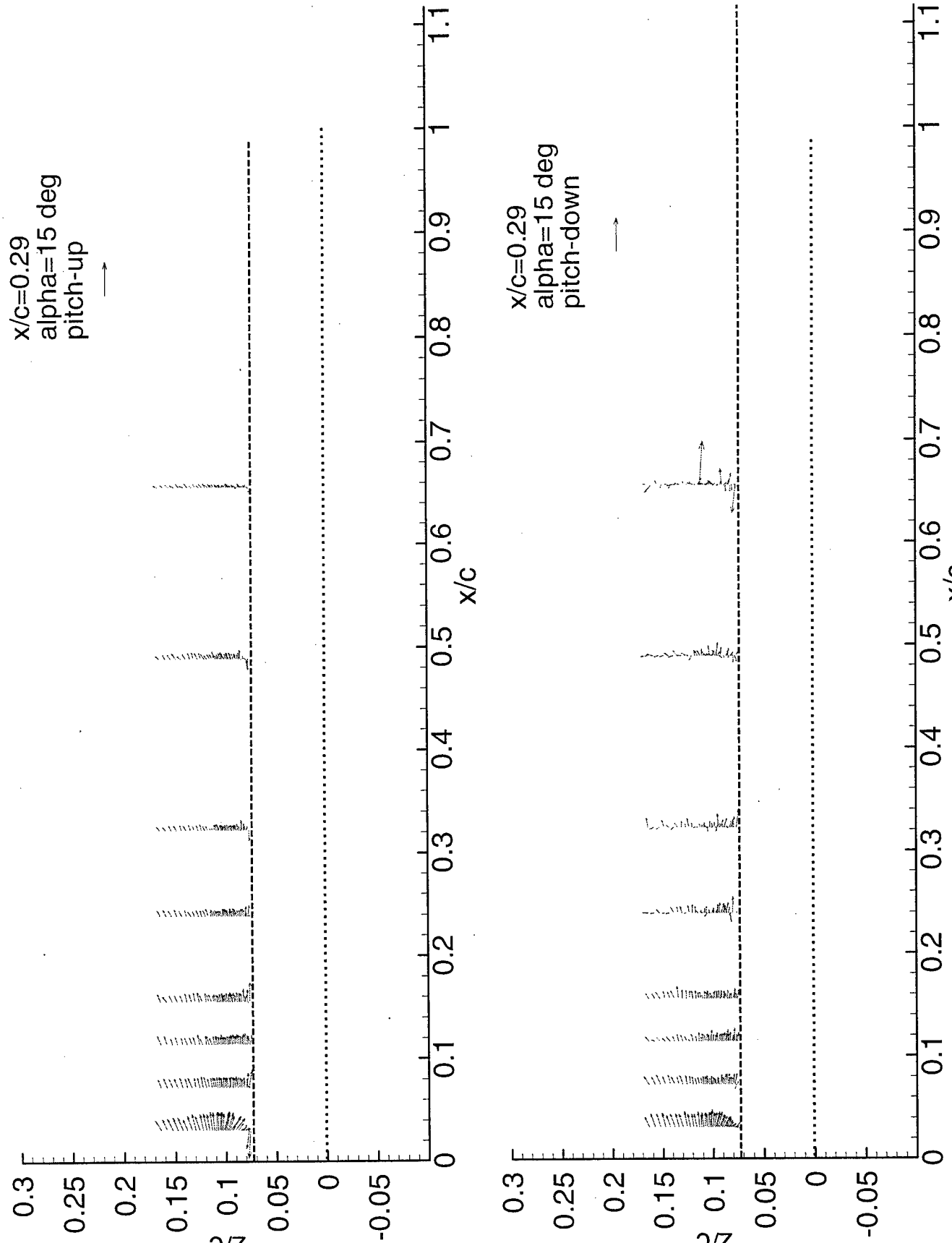

Fig.17 Velocity vectors in the cross-stream plane at x/c=0.29. The reference vector shows magnitude of freestream velocity.

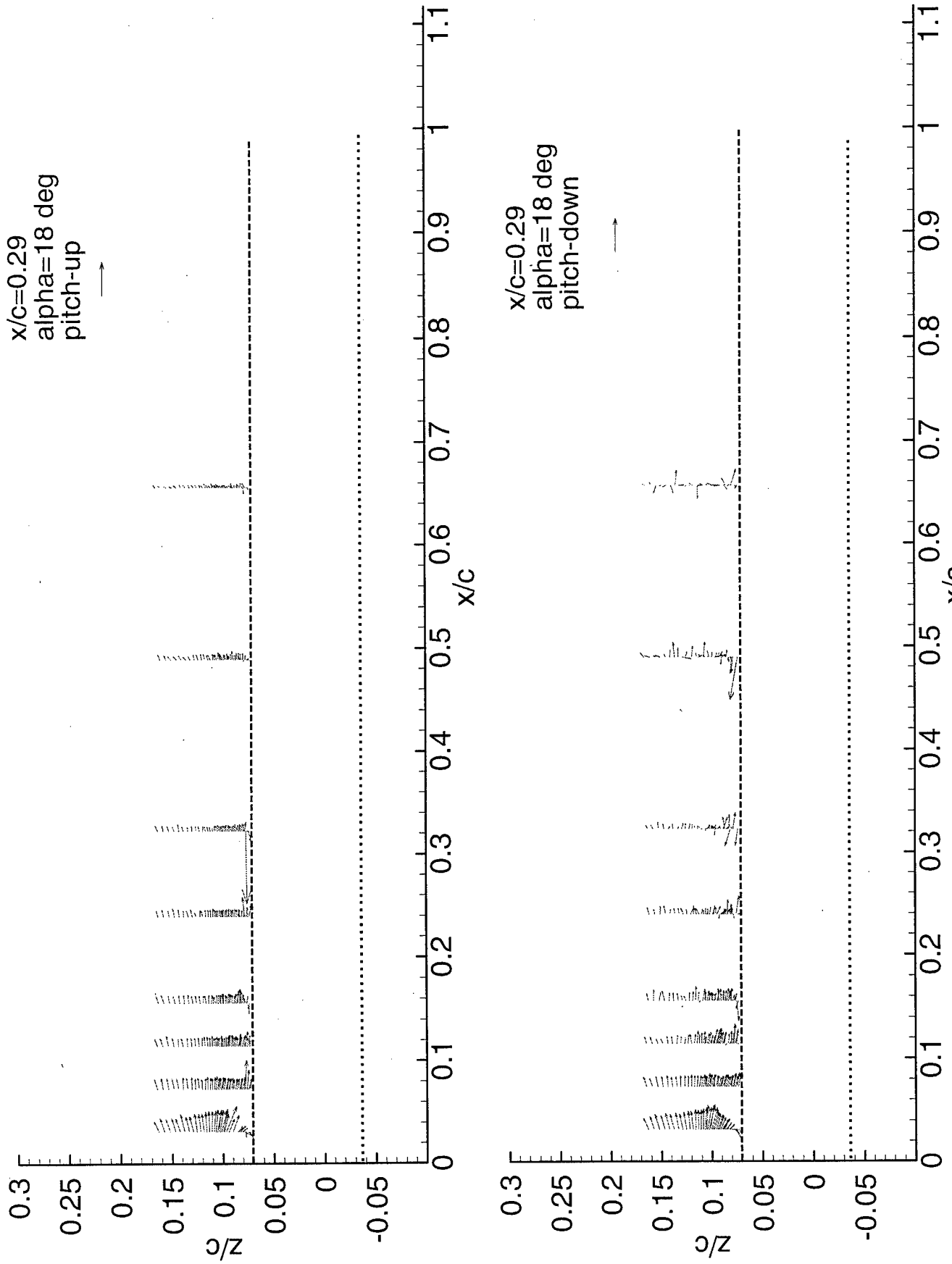

Fig.18 Velocity vectors in the cross-stream plane at x/c=0.29. The reference vector shows magnitude of freestream velocity.

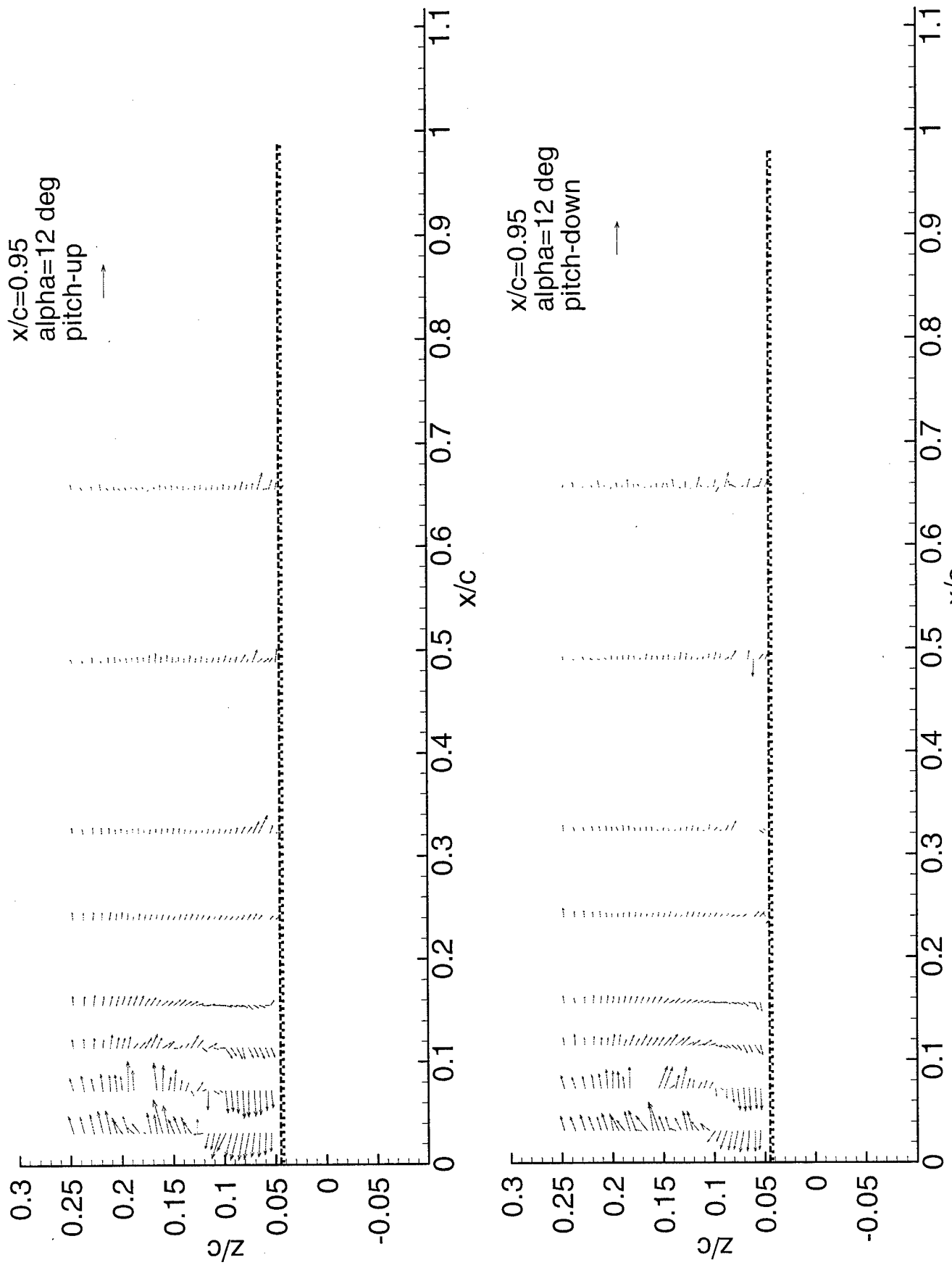

Fig.19 Velocity vectors in the cross-stream plane at x/c=0.95. The reference vector shows magnitude of freestream velocity.

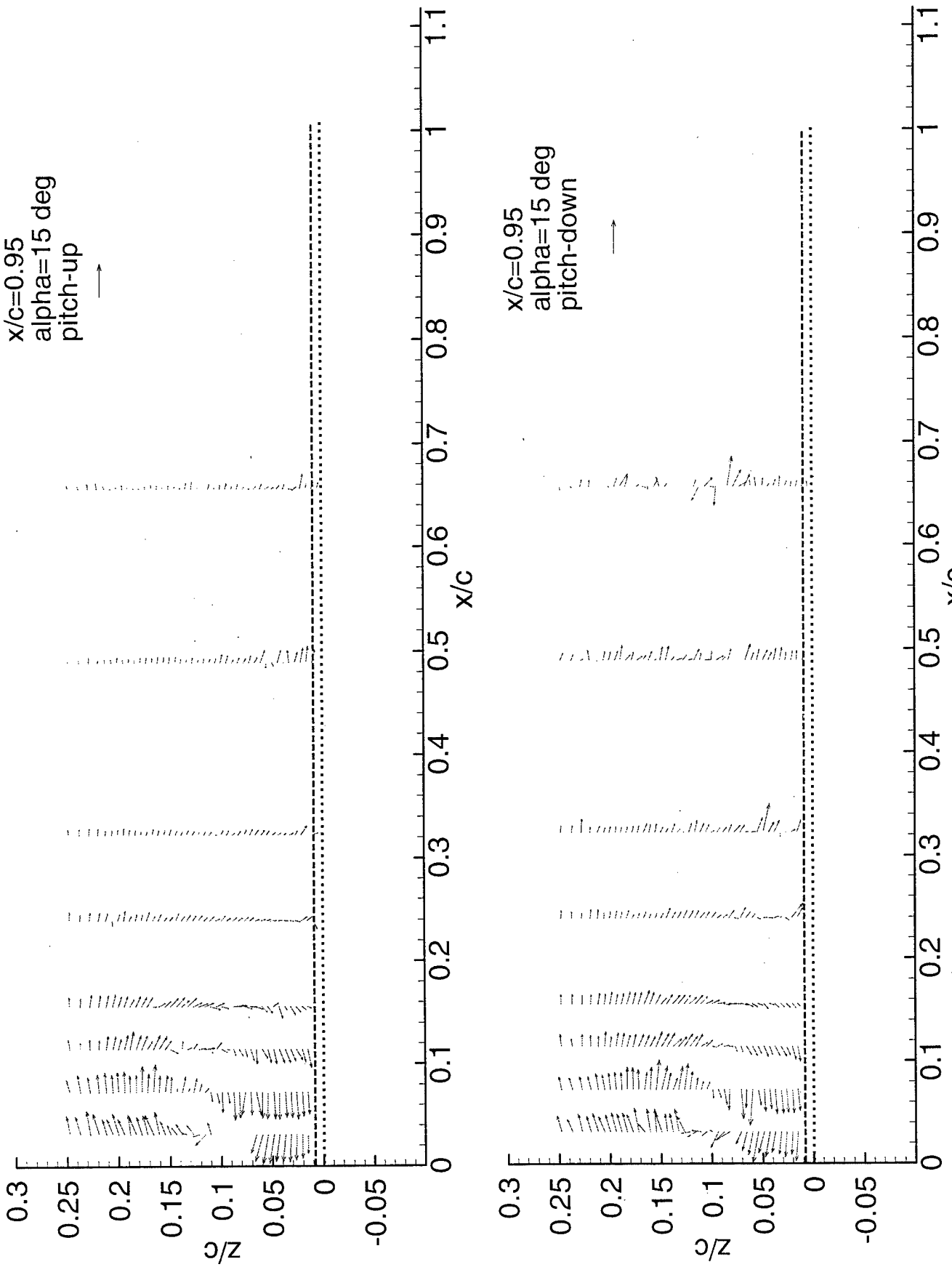

Fig.20 Velocity vectors in the cross-stream plane at x/c=0.95. The reference vector shows magnitude of freestream velocity.

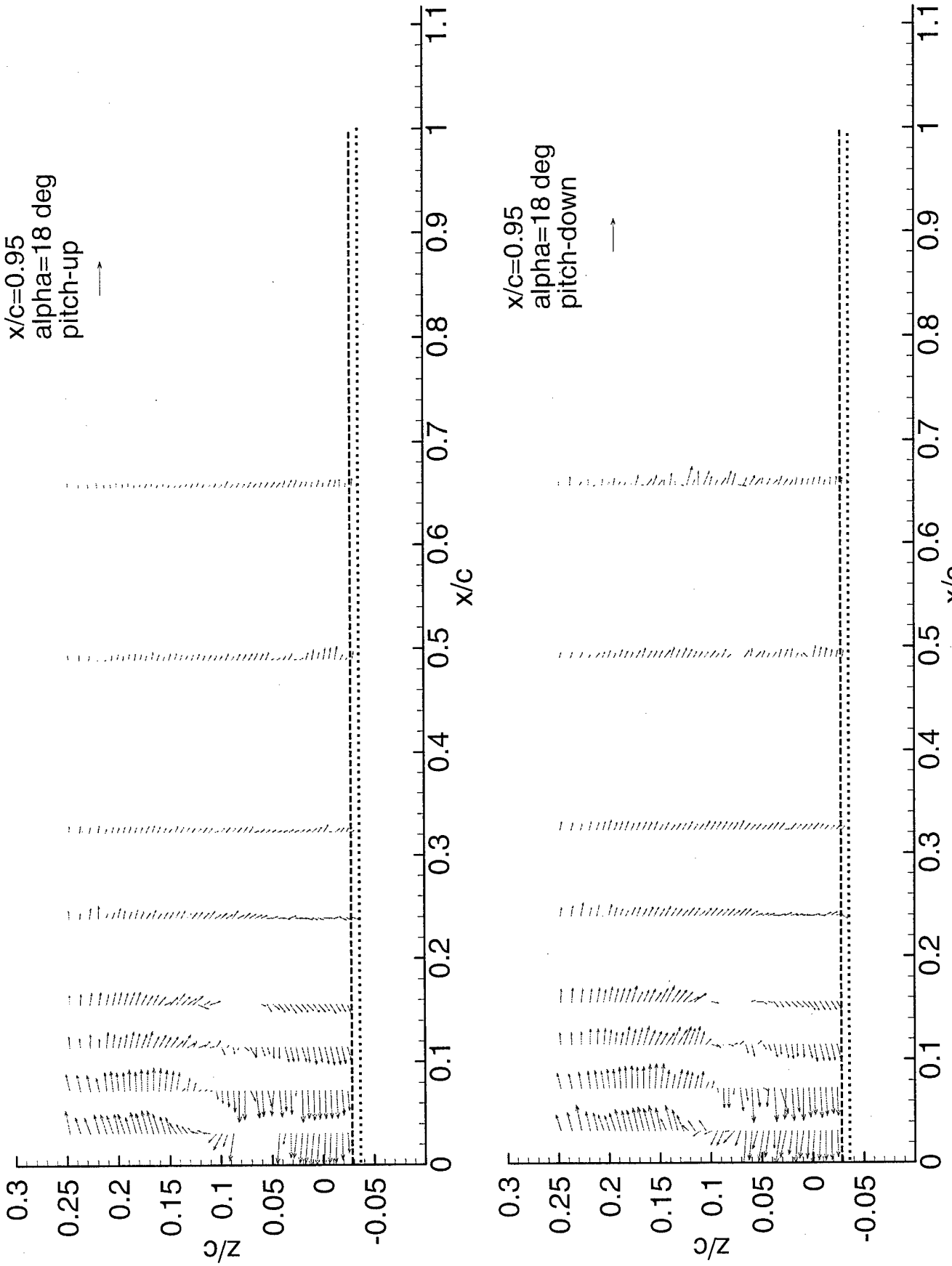

Fig.21 Velocity vectors in the cross-stream plane at x/c=0.95. The reference vector shows magnitude of freestream velocity.

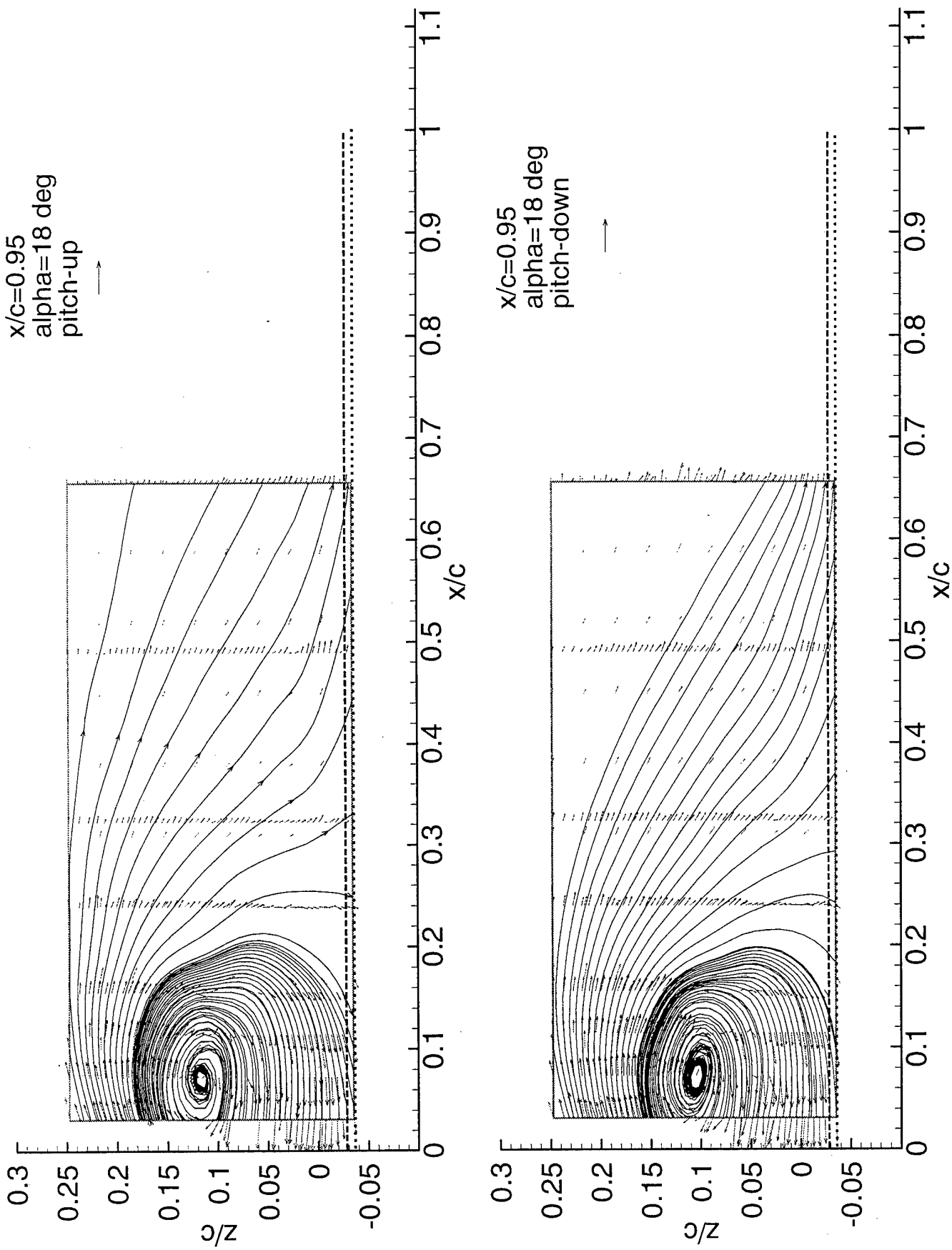

Fig.22 Projection of the streamline traces on the cross-stream plane at x/c=0.95. The light vectors are interpolations from data.